TITLE
ASP Conference Series, Vol. **VOLUME**, **PUBLICATION YEAR**
EDITORS

2dF on the AAT: Current Status and Recent Science Results

Terry Bridges, on behalf of the 2dF Team

Anglo-Australian Observatory, Epping, NSW, Australia

Abstract. I discuss the Two-Degree Field (2dF) multi-fibre spectrograph on the Anglo-Australian Telescope, which reached full operational capability in September 1997. I first give an overview of 2dF, and then show some of the exciting science that has been produced with the instrument. I concentrate on extragalactic science, and focus in particular on some recent results from the 2dF Galaxy Redshift Survey.

1. The 2dF Instrument on the AAT

Full details of 2dF may be found in Lewis et al. (2000, in preparation); see also the 2dF WWW page: http://www.aao.gov.au/2df. 2dF consists of four separate sub-systems:

- **Corrector:** This is a 4-element system, giving a 2 degree field-of-view. It incorporates an Atmospheric Dispersion Compensator (ADC), with rotating prismatic doublets nearly a metre across.
- **Fibre Positioner and Optical Fibres:** There are two field plates, each with 400 object fibres and an additional 4 guide fibre bundles. The fibres are 140 μm in diameter ($\sim$ 2.1 arcsec). A novel feature of 2dF is the tumbler arrangement, whereby one field is configured with a robotic positioner, while the second plate is being observed. When the field set-up is complete, the tumbler rotates so that the observing plate now becomes the configuring plate (and vice-versa).
- **Spectrographs:** There are two spectrographs, each receiving 200 fibres. The f/1.2 camera is a modified Schmidt design using a single, severely aspheric corrector plate. The 2dF gratings range from 270 to 1200 lines/mm, giving resolutions between 2.5−12 Ang. The detectors are 1024^2 thinned Tektronix CCDs; with 200 spectra on each detector the spectra are spaced roughly 5 pixels apart.
- **Software:** Just as important as the 2dF hardware is the associated software. In addition to control software, there is custom-built software for configuring fields (`Configure`) and reducing 2dF data (`2dfdr`).

Figure 1 is a schematic of 2dF on the telescope, while Table 1 lists the important attributes of 2dF.

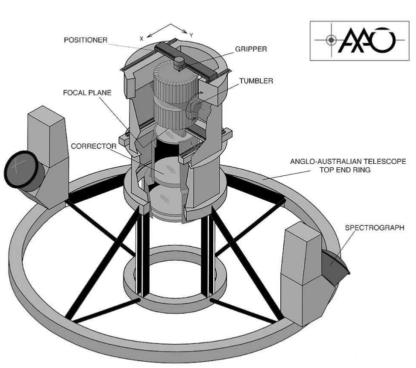

Figure 1. Schematic of 2dF on the AAT top end.

Table 1. Main Parameters of 2dF

Field of View	2 deg
Number of Fibres	400 object fibres + 4 guide bundles on each plate
Fibre Diameter	140 μm $\simeq 2.1''$
Configuration Time	$\sim$ 7 sec/fibre ($\sim$ 65 min/field)
Fibre Positioning Accuracy	20 μm $\simeq 0.3''$
Spectral Resolution	2.5 Å (1200 l/mm)– 12 Å (270 l/mm)
Total System Throughput	$\sim$ 0.05
Limiting Magnitude[1]	B $\simeq$ 22

[1] assumes: point source, $1.5''$ seeing, low dispersion, 4 hour integration, S/N=10

2. 2dF Science

I don't have space here to discuss all of the wonderful science that has been obtained with 2dF. Instead, I present only a few examples, concentrating on extragalactic programmes, and the 2dF Galaxy Redshift Survey in particular. Please see the November 1999 AAO Newsletter for more 2dF science (http://www.aao.gov.au/AAO/local/www/lib/newsletters/nov99/nov99.htm).

2.1. Intracluster Planetary Nebulae in the Virgo Cluster

K. Freeman, M. Arnaboldi, M. Capaccioli, et al. 2000

Planetary nebulae (PNe) have been used for several years to study the dynamics of early-type galaxies. More recently, intracluster PNe in the Virgo and Fornax clusters (ie., those not attached to individual galaxies) have been used to study the intracluster environment and cluster potential.

Freeman et al. have used narrow-band imaging to identify a sample of candidate intracluster PNe in the Virgo cluster. 110 PNe candidates were observed with 2dF in March 1999 with the 1200V gratings, yielding 47 detections. Of these, 23 are genuine intracluster PNe, 16 were found in the outer regions of M87, and 8 are likely to be background galaxies at z $\simeq$ 3.1 (Lyα shifting to $\sim$ 5000 Å). **Figure 2** shows the sum of 23 intra-cluster PNe. For the 23 confirmed

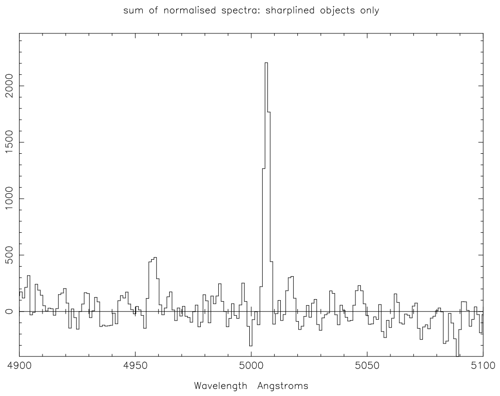

Figure 2. Summed 2dF spectrum of 23 intracluster PNe candidates in the Virgo cluster. (Freeman et al. 2000)

intracluster PNe, the average velocity is 1193 ± 15 km/sec and the velocity dispersion is $\sigma = 752 \pm 110$ km/sec; these are in agreement with those for Virgo cluster galaxies. See Freeman et al. (2000) for more information.

2.2. Galaxy-Galaxy Gravitational Lensing

J. Willis, P. Hewett, S. Warren, & G. Lewis 2000

Willis et al. have developed an alternative strategy for finding galaxy-galaxy gravitational lenses. From $B_J RI$ APM plates, they identify a population of massive early-type galaxies at z ~ 0.4, which are an almost ideal population of deflectors. Background lensed galaxies are then revealed by the detection of anomalous emission lines in the deflector spectra.

In September 1998, Willis et al. obtained spectra of ~ 500 early-type galaxies in two nights with 2dF, with exposure times of ~ 8000 sec per field. They were able to measure redshifts in 95% of the deflector galaxies and are sensitive to anomalous emission lines with fluxes $\geq 5 \times 10^{-17}$ erg/sec/cm^{-}2. **Figure 3** shows their spectra ordered by increasing redshift. Subsequent analysis has revealed four anomalous emission lines, consistent with gravitationally-lensed Lyman-α emission. These will be followed up with further spectroscopy and high-resolution imaging. See Willis et al. (2000) for further details.

2.3. The 2dF Galaxy Redshift Survey

The 2dF Galaxy Redshift Survey (2dFGRS) aims to obtain spectra and redshifts for ~ 250,000 galaxies with $b_j < 19.5$. The survey covers a region of ~ 1700 deg^2 in two strips centered at the equator and -30 declination. As of October 2000, the 2dFGRS had collected just under 130,000 redshifts. For more information about the survey, see: http://www.mso.anu.edu.au/2dFGRS/, and also **Other Ref here**.

The goals of the survey are many, covering topics in large-scale structure, cosmology, galaxy formation, galaxy clusters and groups, and galactic stellar populations. Here I focus on three recent results; these are all preliminary and may change in the final published versions.

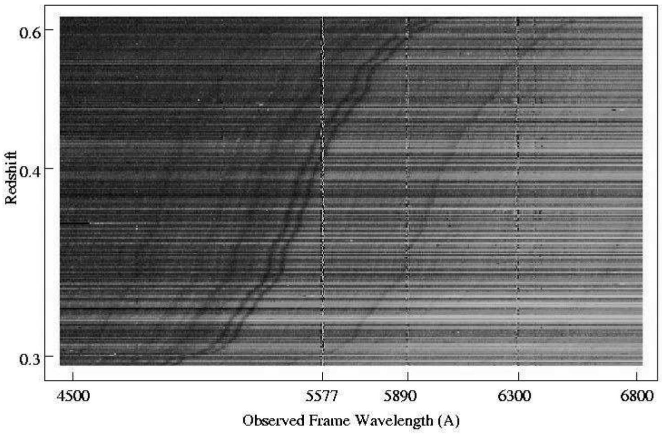

Figure 3. Observed-frame spectra of 485 early-type galaxies with $0.3 \leq z \leq 0.6$, arranged by increasing redshift. Strong night-sky features are visible as vertical lines while intrinsic features (e.g. Ca H&K, G-band) move to longer wavelength as z increases. (Willis et al. 2000)

(1) Catalogued Clusters in the 2dFGRS

R. De Propris et al. 2000, submitted to MNRAS

De Propris et al. have carried out a study of known clusters with the 2dF-GRS, and have identified 207 Abell clusters, 54 APM, and 167 EDCC clusters. Redshifts and velocity dispersions have been measured for these clusters, and used to study the contamination of the cluster catalogues, and the space density of the clusters with redshift.

The distribution of cluster velocity dispersions puts constraints on cosmological models of structure formation. **Figure 4** shows the cluster velocity dispersion distribution from De Propris et al. The most striking aspect is the lack of high σ clusters. De Propris et al. derive an upper limit of 2.5×10^{-6} h^{-1} Mpc^{-3} for the space density of clusters with $\sigma > 1000$ km/sec, which is most consistent with a low matter density, $\Omega_M < 0.4$.

(2) Infrared Galaxy Luminosity Functions

S. Cole et al. 2000, submitted to MNRAS

Cole et al. have combined the 2MASS extended source catalogue and the 2dFGRS to produce an IR-selected galaxy catalogue with nearly 13,000 measured redshifts (an order of magnitude larger than previous datasets). Study of the near-IR properties of galaxies is useful because near-IR luminosities are directly related to the underlying stellar mass and integrated star formation histories of galaxies, and place strong constraints on galaxy formation models.

Cole et al. use their combined catalogue to determine J and K_S band luminosity functions (LFs); **Figure 5** shows the K_S LF. Using the K_S LF and simple galaxy evolutionary models, they derive the galactic stellar mass function. Integrated over all galaxy masses, this gives a total mass fraction in stars of $\Omega_{stars} = 0.0014 \pm 0.0001$ and 0.0029 ± 0.0003 for Kennicutt and Salpeter IMFs, respectively.

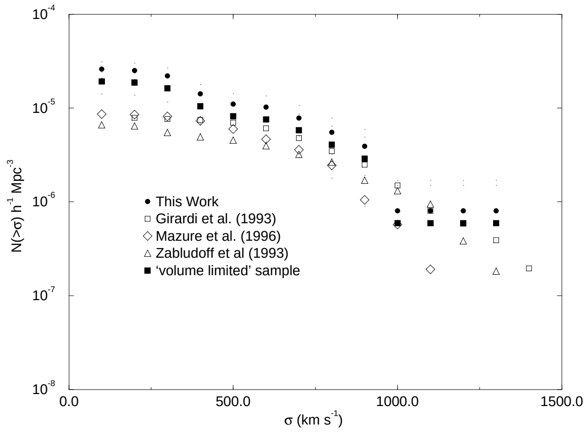

Figure 4. Velocity dispersion distribution for clusters in the 2dF Galaxy Redshift Survey, and from previous work (De Propris et al. 2000).

(3) Measuring the Cosmological Density with the 2dFGRS

J. Peacock et al. 2000, submitted to Nature

The combination of Hubble expansion and systematic infall due to large-scale structure causes an apparent flattening of structures along the radial direction, and anisotropy in the inferred spatial clustering of galaxies. This effect can be used to determine the distortion parameter $\beta \equiv \Omega_M^{0.6}/b$, where Ω_M is the total matter density and b is the usual bias parameter of optical galaxies.

Peacock et al. have used $\sim$ 113,000 2dFGRS redshifts to derive the redshift-space correlation function $\xi(\sigma, \pi)$, which measures the probability over random of finding a pair of galaxies with transverse separation σ and line-of-sight separation π; this is shown in **Figure 6**. The flattening on large scales is clearly seen in this figure, and yields $\beta = 0.39 \pm 0.05$. Comparison with the analysis of CMB anisotropies implies a low-density universe with $\Omega_M \simeq 0.35$.

3. The Future: AAΩ

AAΩ will be the next generation optical spectrograph for the AAT. Based on 2dF, new optical fibres and a powerful integral field unit (IFU) will feed new bench-mounted spectrographs. At the time of writing, **AAΩ** is in the conceptual design phase, and is estimated to be on the telescope in 2003.

Acknowledgments. 2dF science would not be possible without the hard work of a large number of AAO staff in the designing, building, and maintaining of 2dF. I'm grateful to Ken Freeman, Paul Hewett, and the 2dF Galaxy Redshift Survey Team, in particular Shaun Cole, Roberto De Propris, and John Peacock, for allowing me to present their science and for sending me figures.

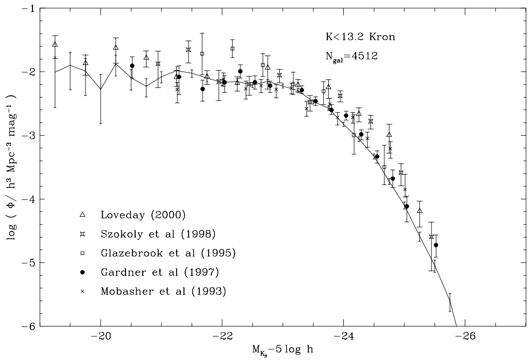

Figure 5. The solid line shows a Step Wise Maximum Likelihood estimate of the K_S-band luminosity function (Kron magnitudes) for the combined dataset of $\sim$ 13,000 galaxies from the 2dF Galaxy Redshift Survey and the 2MASS extended source catalogue. The other symbols and errorbars are as indicated on the plot. (Cole et al. (2000)

References

Freeman, K. et al. 2000, in *"Galaxy Dynamics: From the Early Universe to the Present"*, ASP Conf. Ser. (astroph/9910057)

Willis, J.P., et al. 2000, in "Proceedings of the XXth Moriond Astrophysics Meeting: *Cosmological Physics with Gravitational Lensing*" (astro-ph/0008068)

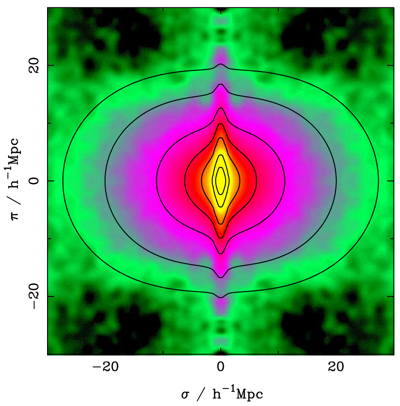

Figure 6. The redshift-space correlation function for the 2dF Galaxy Redshift Survey, $\xi(\sigma,\pi)$, as a function of transverse (σ) and radial (π) pair separation. The plot clearly shows redshift distortions, with 'fingers of God' elongations at small scales, and flattening at large radii from systematic infall. The overplotted contours show model predictions with flattening parameter $\beta \equiv \Omega^{0.6}/b = 0.4$ and a pairwise dispersion of $\sigma_p = 4\ h^{-1}$ Mpc. Contours are plotted at ξ=10,5,2,1,0.5,0.2,0.1.